Electronic Supplementary Material (ESI) for Dalton Transactions.
This journal is © The Royal Society of Chemistry 2024

## Supporting Information Available

# Novel half Salphen cobalt(III) complexes: synthesis, DNA binding and anticancer studies

Riccardo Bonsignore,[a*] Elisa Trippodo,[a] Roberto Di Gesù,[b] Anna Paola Carreca,[b] Simona Rubino,[a] Angelo Spinello,[a] Alessio Terenzi,[a] Giampaolo Barone.[a*]

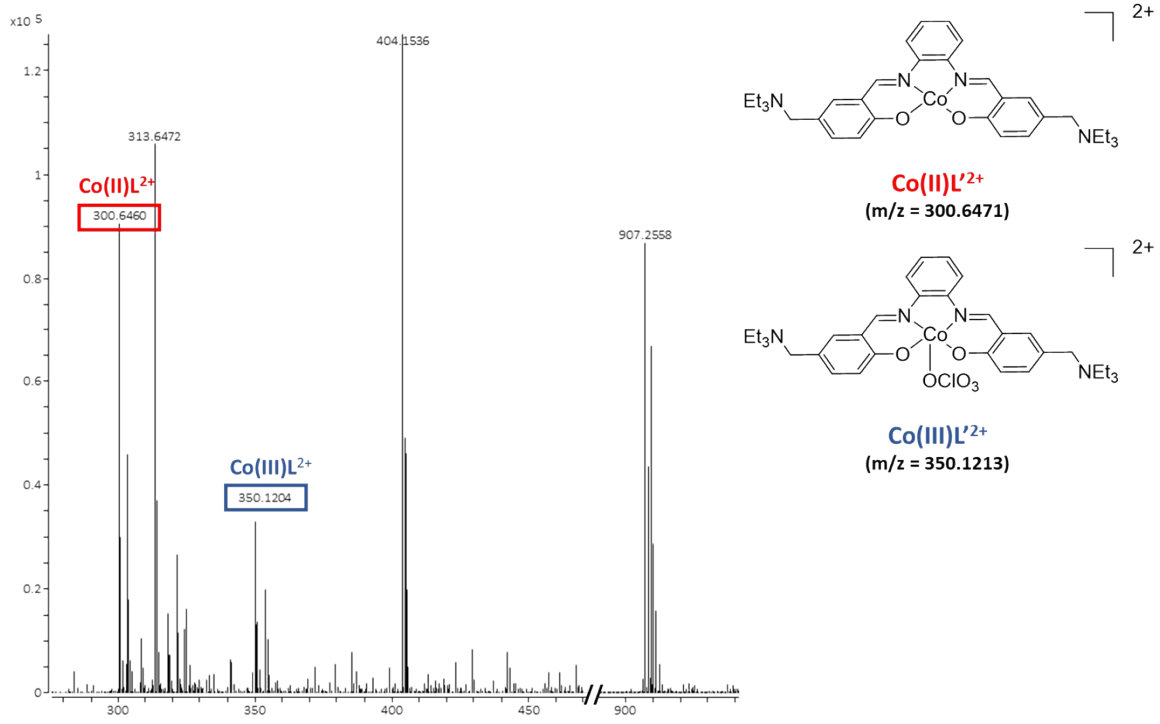


**Figure S1.** ESI-MS spectrum in acetonitrile of the pH = 6 reaction.

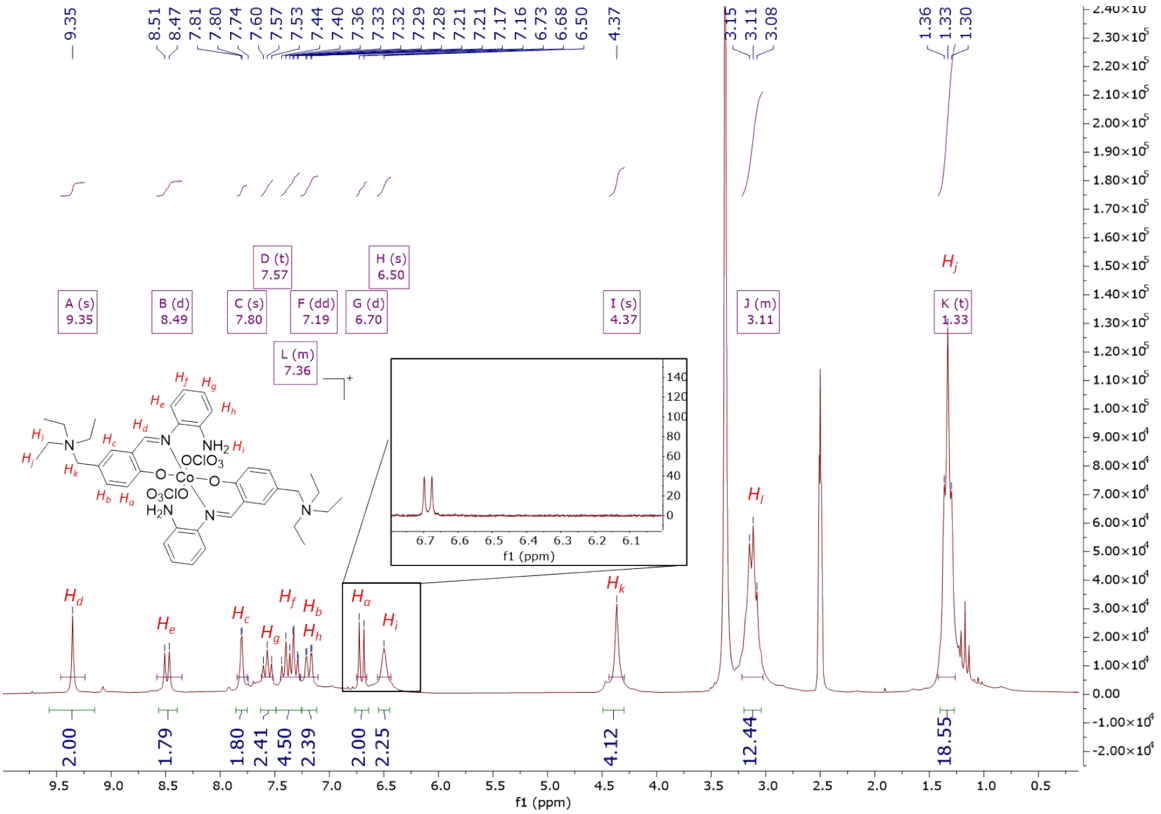


**Figure S2.** $^{1}$H NMR of **1** in *d*6-DMSO. In the inset, $H_k$ signal disappearance upon $D_2O$ addition.

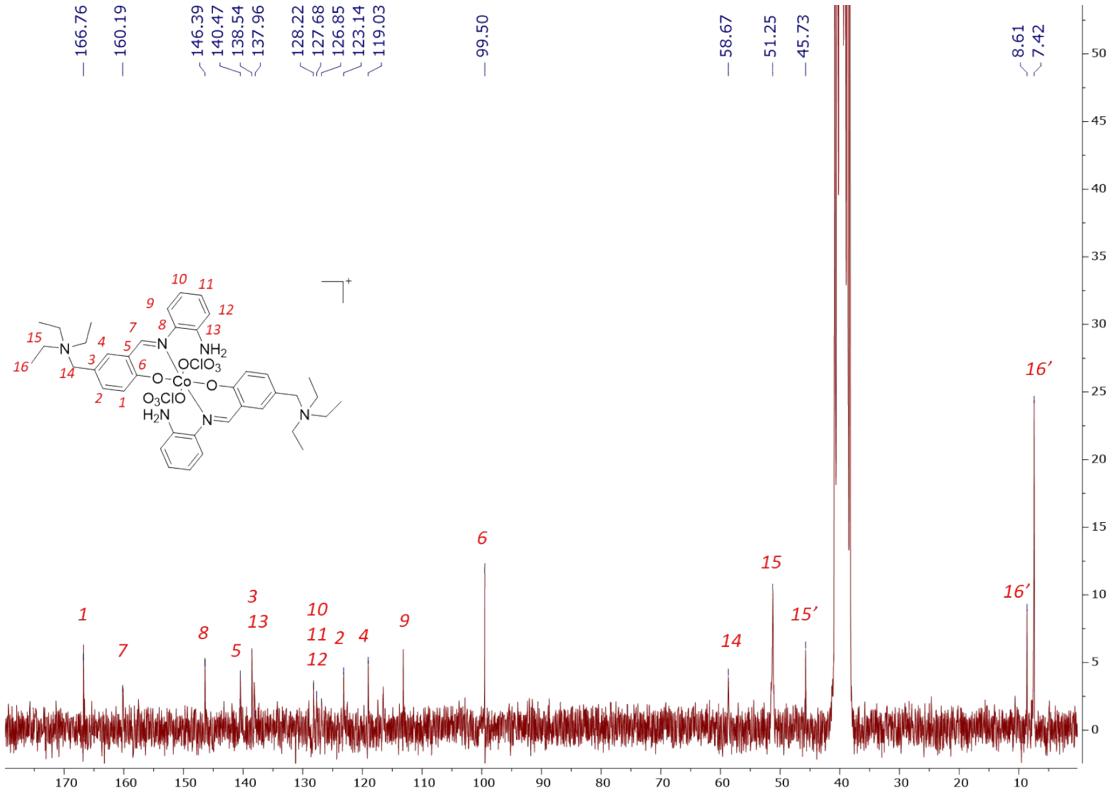


**Figure S3.** $^{13}$C NMR of **1** in *d*6-DMSO.

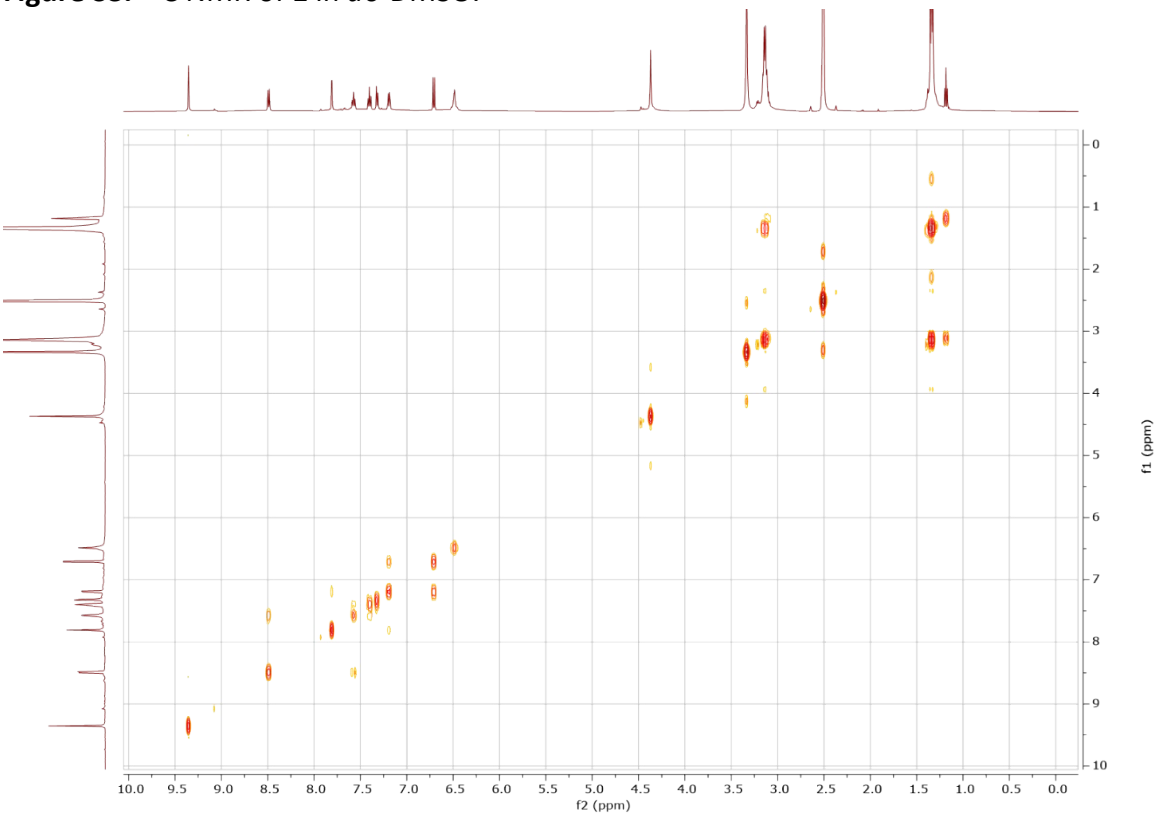


**Figure S4.** $^{1}$H-$^{1}$H COSY NMR of **1** in *d*6-DMSO.


**Figure S5.** $^{1}H$-$^{13}C$ HSQC NMR of **1** in *d*6-DMSO.

**a)**

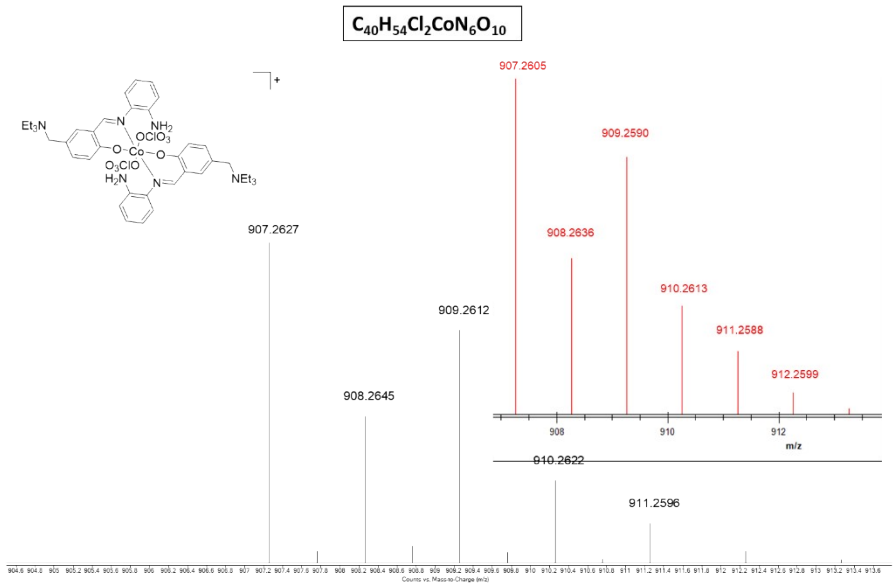

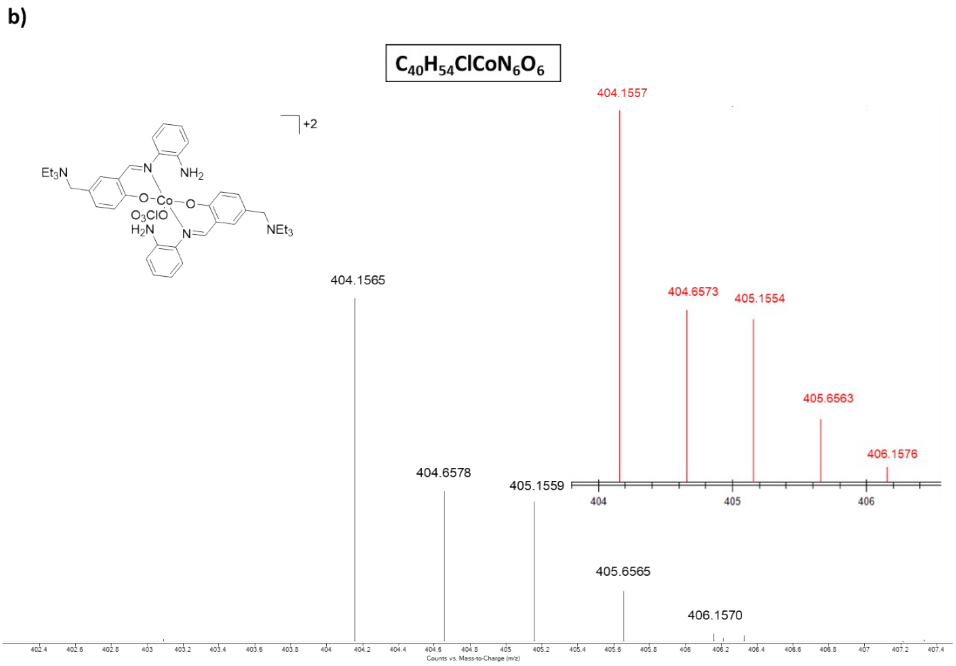


**Figure S6.** ESI-MS spectra of the two species found for **1** in acetonitrile: $[\mathbf{1}]^{+}$ (a) and $[\mathbf{1}\text{-}\mathbf{ClO_4}]^{+2}$ (b). Simulated specta are depicted in red as insets.

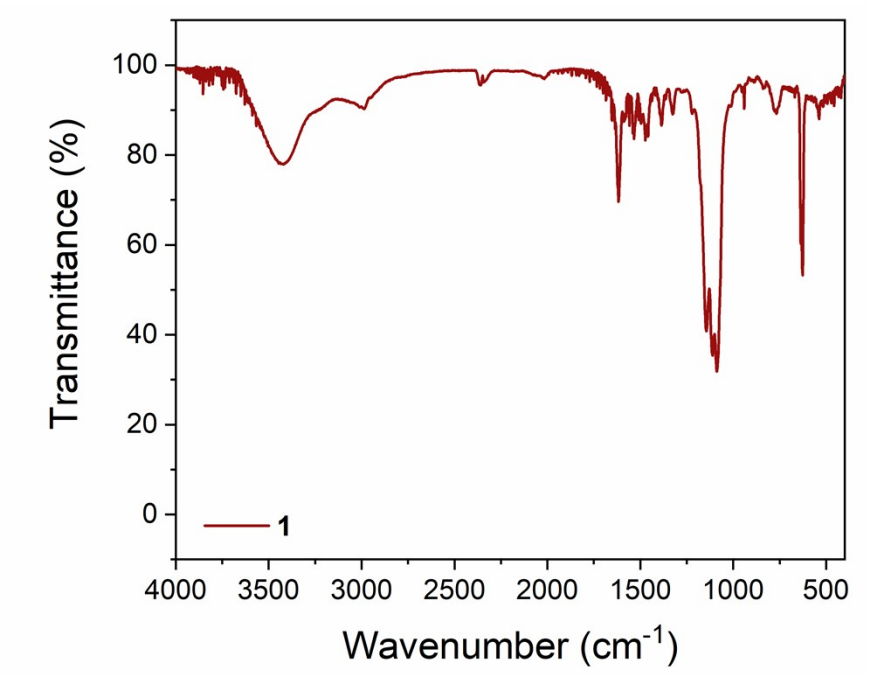


**Figure S7.** IR spectrum of **1** in KBr.

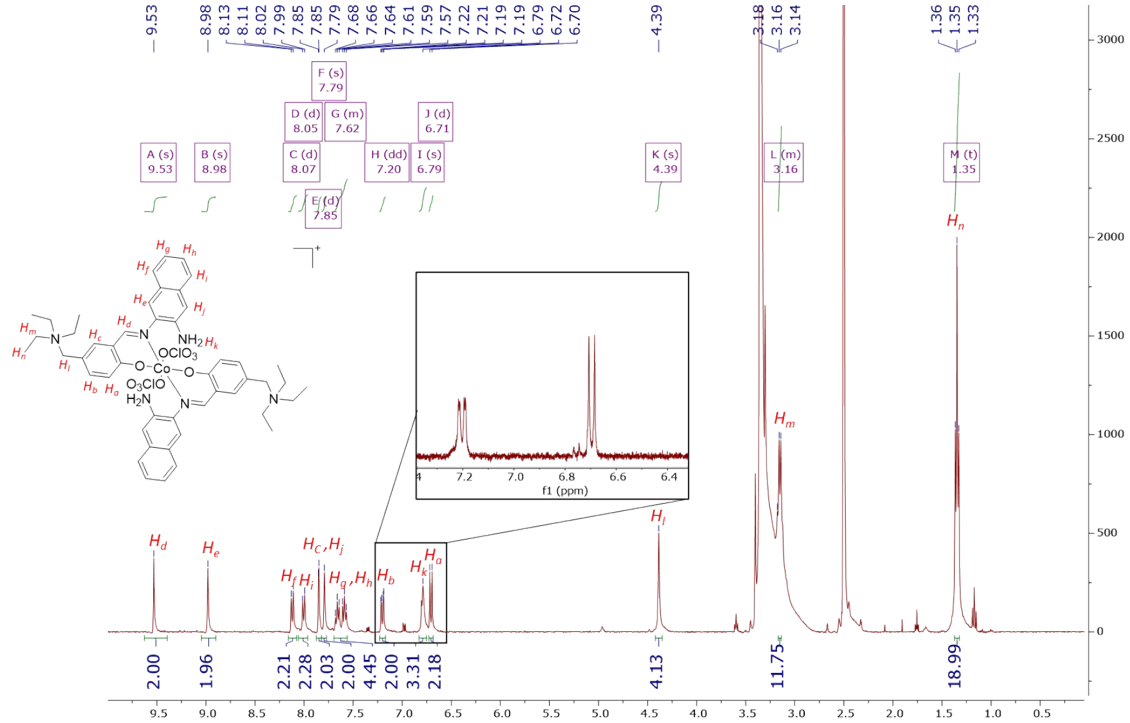

**Figure S8.** $^{1}$H NMR of **2** in *d*6-DMSO. In the inset, $H_k$ signal disappearance upon $D_2O$ addition.

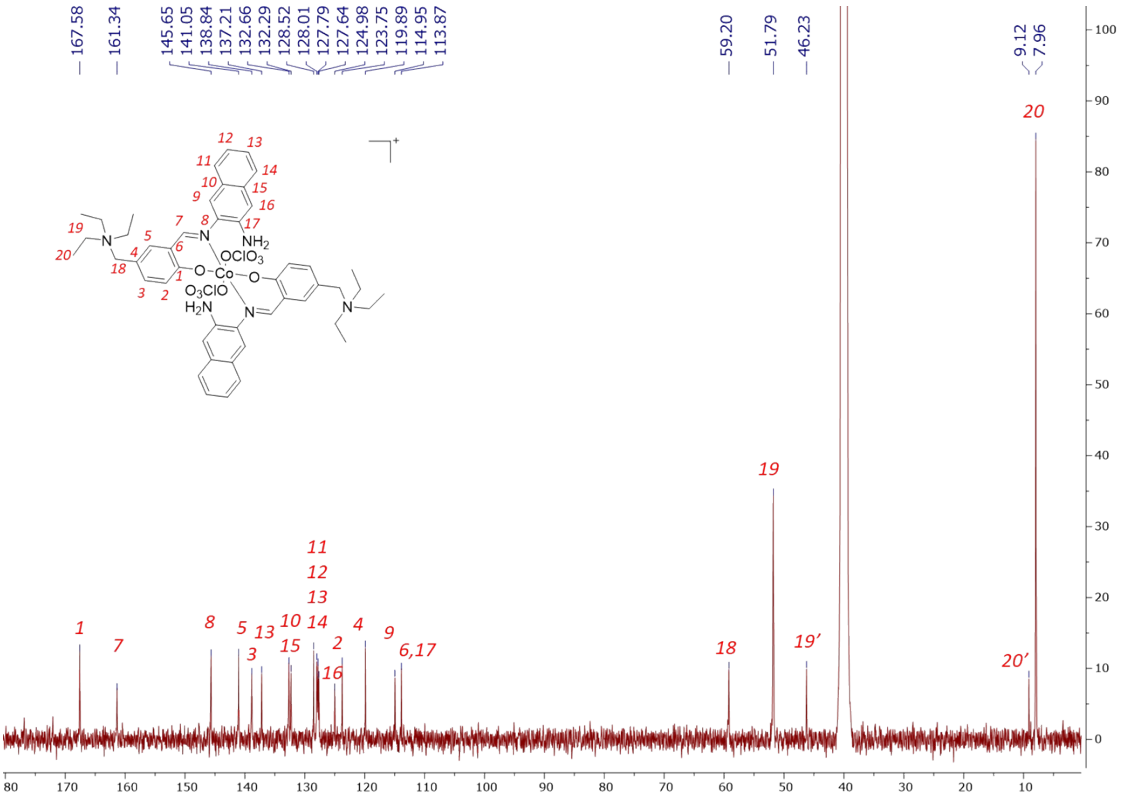

**Figure S9.** $^{13}$C NMR of **2** in *d*6-DMSO.

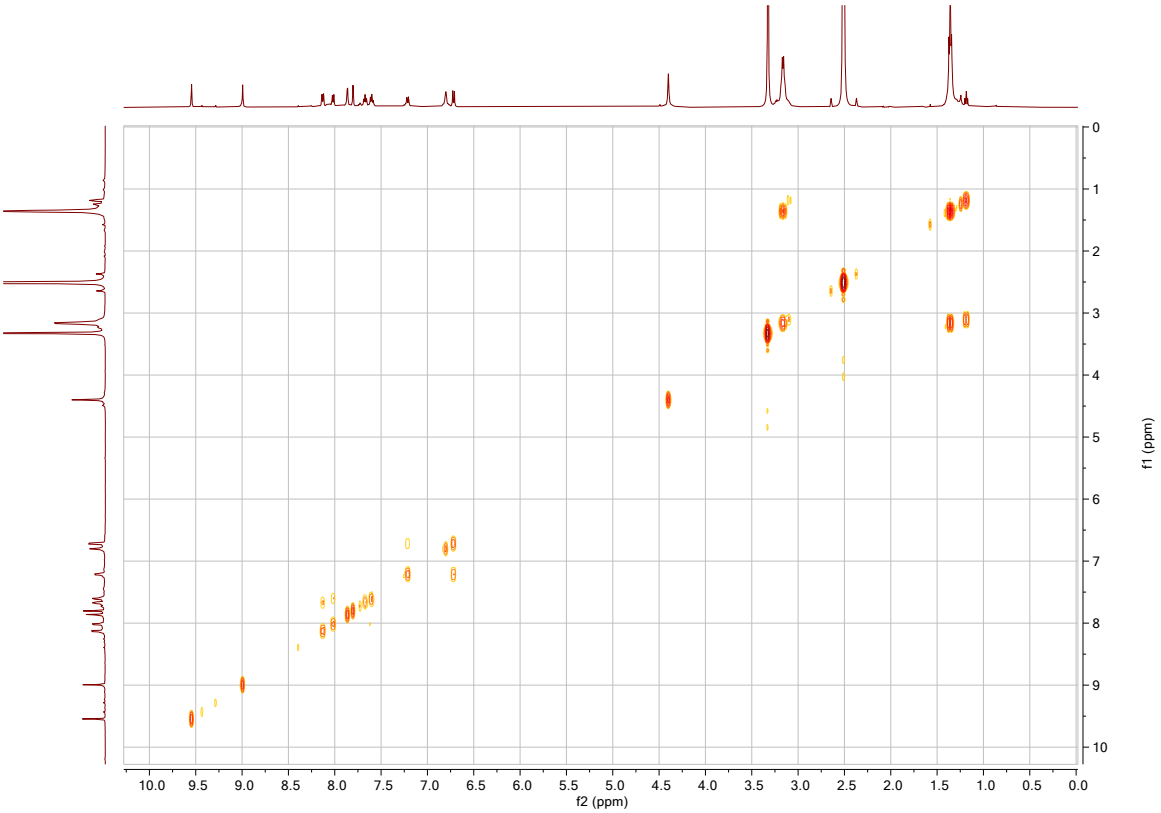


**Figure S10.** $^{1}$H-$^{1}$H COSY NMR of **2** in *d*6-DMSO.

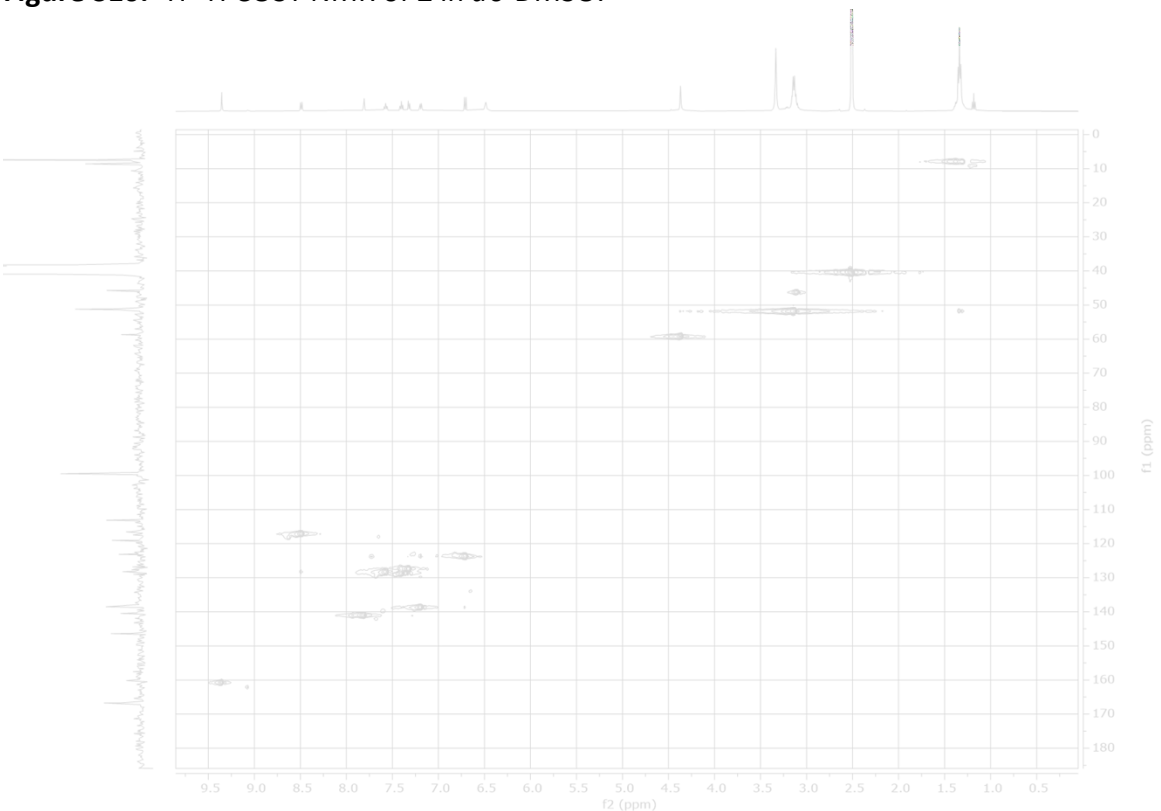


**Figure S11.** $^{1}$H-$^{13}$C HSQC NMR of **1** in *d*6-DMSO.

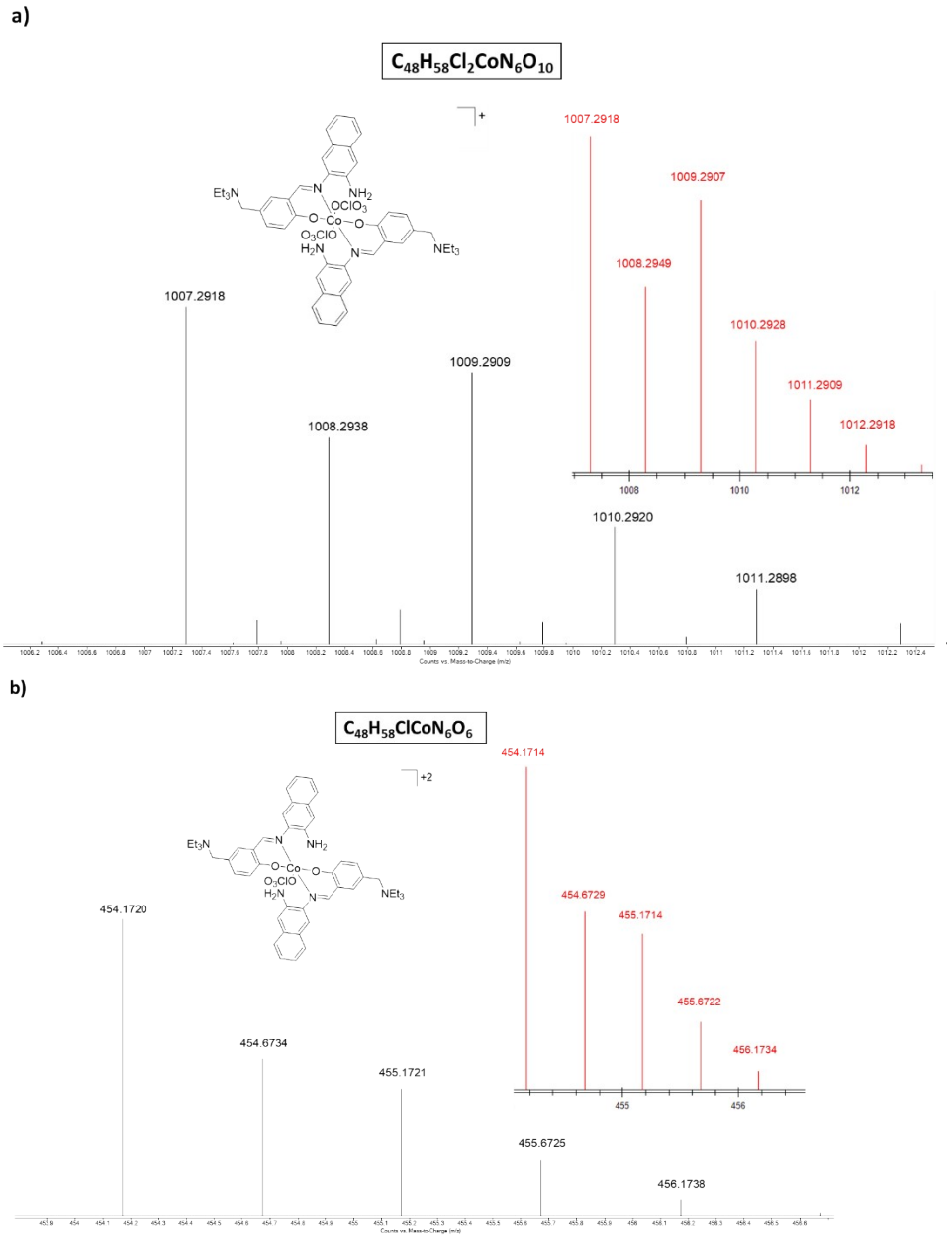


**Figure S12.** ESI-MS spectra of the two species found for **2** in acetonitrile: $[\mathbf{2}]^{+}$ (a), $[\mathbf{2\text{-}ClO_4}]^{+2}$ (b). Simulated specta are depicted in red as insets.

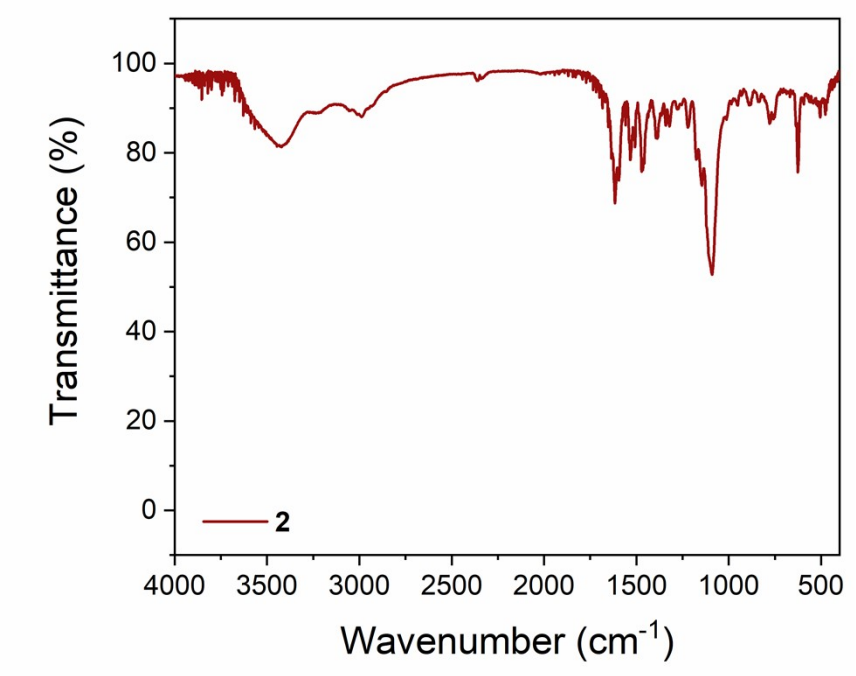


**Figure S13.** IR spectrum of **2** in KBr.

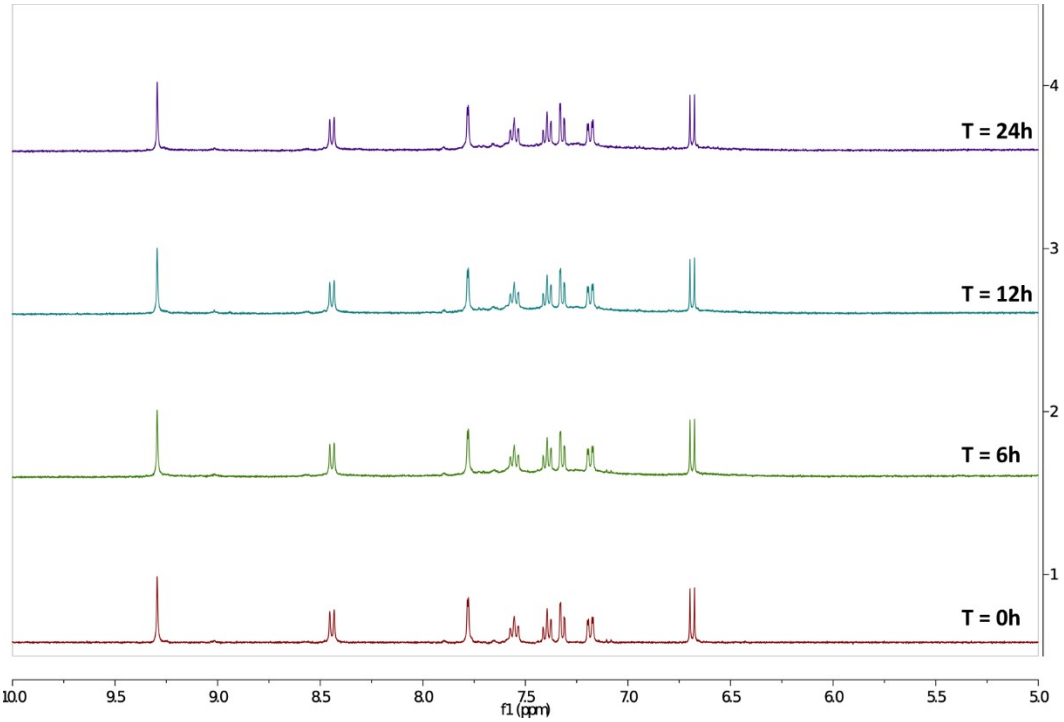


**Figure S14.** $^{1}H$ NMR stability studies of **1** in *d*6-DMSO:$D_2O$ (80:20) over 24 h. The selected timepoints are reported on the right.

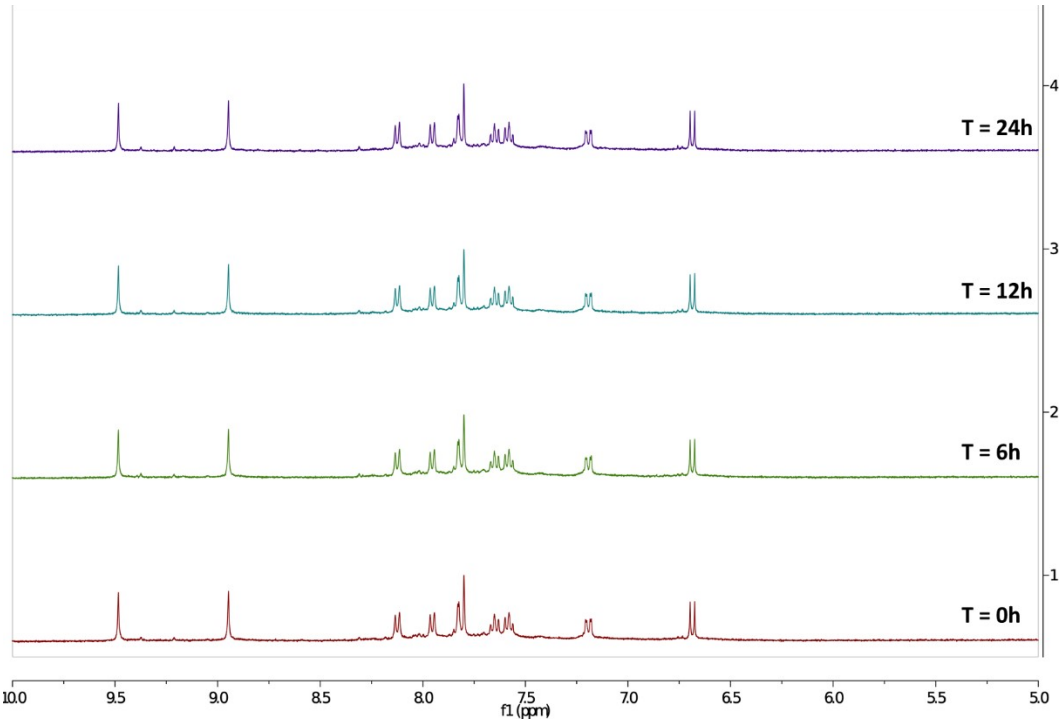


**Figure S15.** $^{1}$H NMR stability studies of **2** in *d*6-DMSO:$D_2O$ (80:20) over 24 h. The selected timepoints are reported on the right.

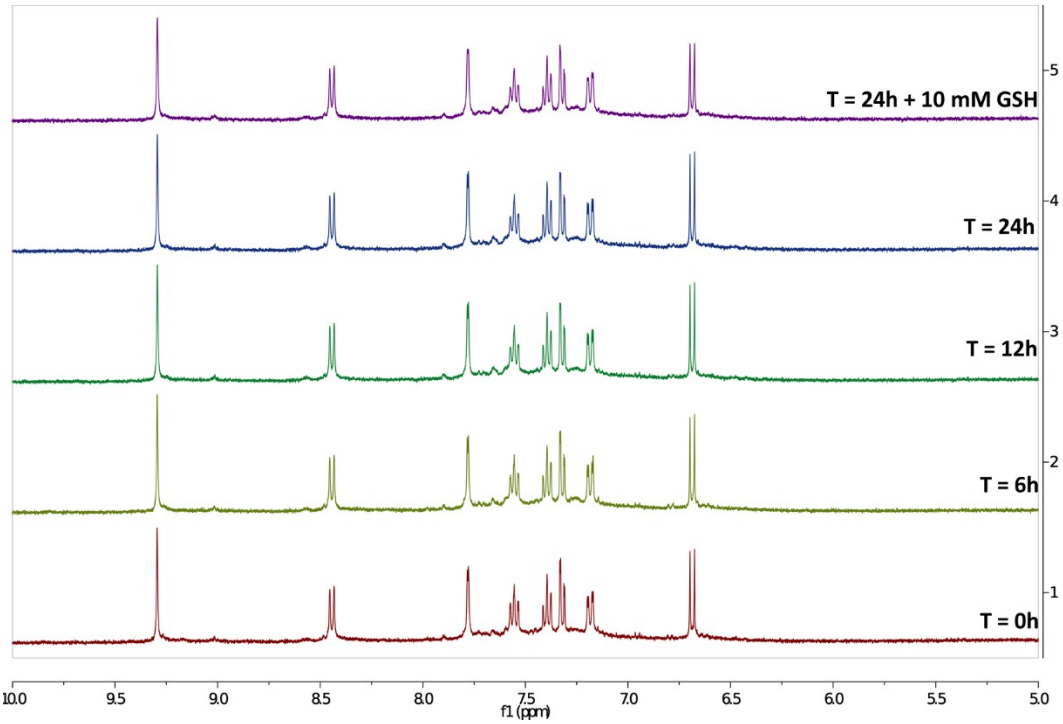


**Figure S16.** $^{1}$H NMR stability studies of **1** recorded over 24 h in a 2 mM GSH *d*6-DMSO:$D_2O$ (80:20) mixture. In the top spectrum, $^{1}$H NMR stability studies of **1** in the presence of an excess of GSH (10 mM), collected in the same solvent as above. The selected timepoints are reported on the right.

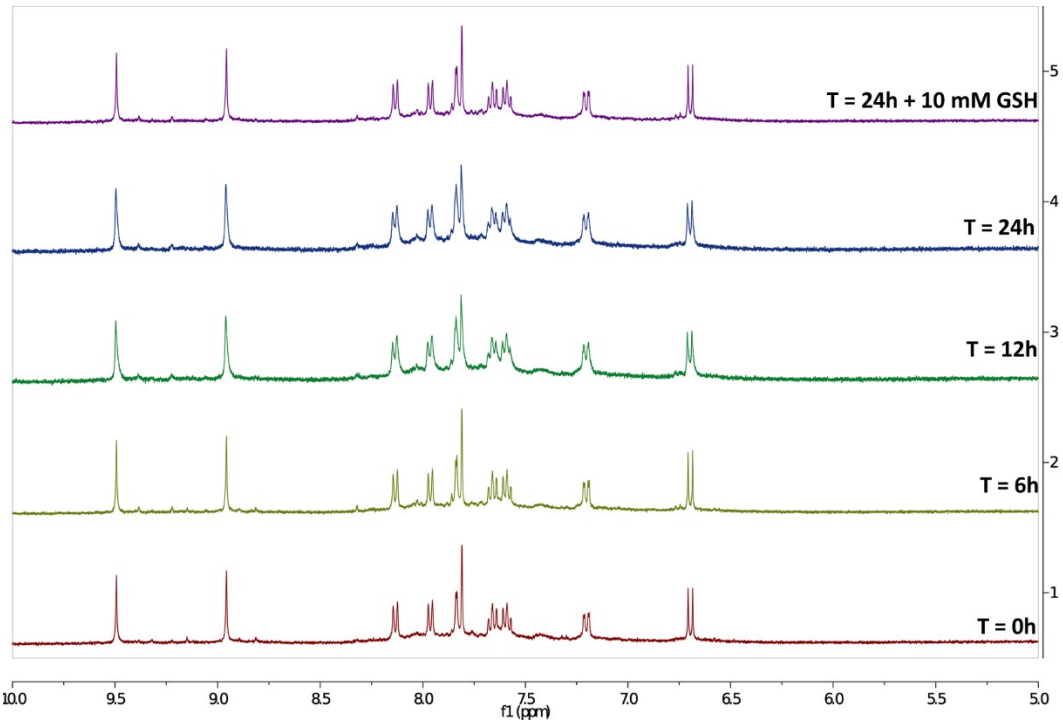


**Figure S17.** $^{1}$H NMR stability studies of **2** recorded over 24 h in a 2 mM GSH *d*6-DMSO:$D_2O$ (80:20) mixture. In the top spectrum, $^{1}$H NMR stability studies of **1** in the presence of an excess of GSH (10 mM), collected in the same solvent as above. The selected timepoints are reported on the right.

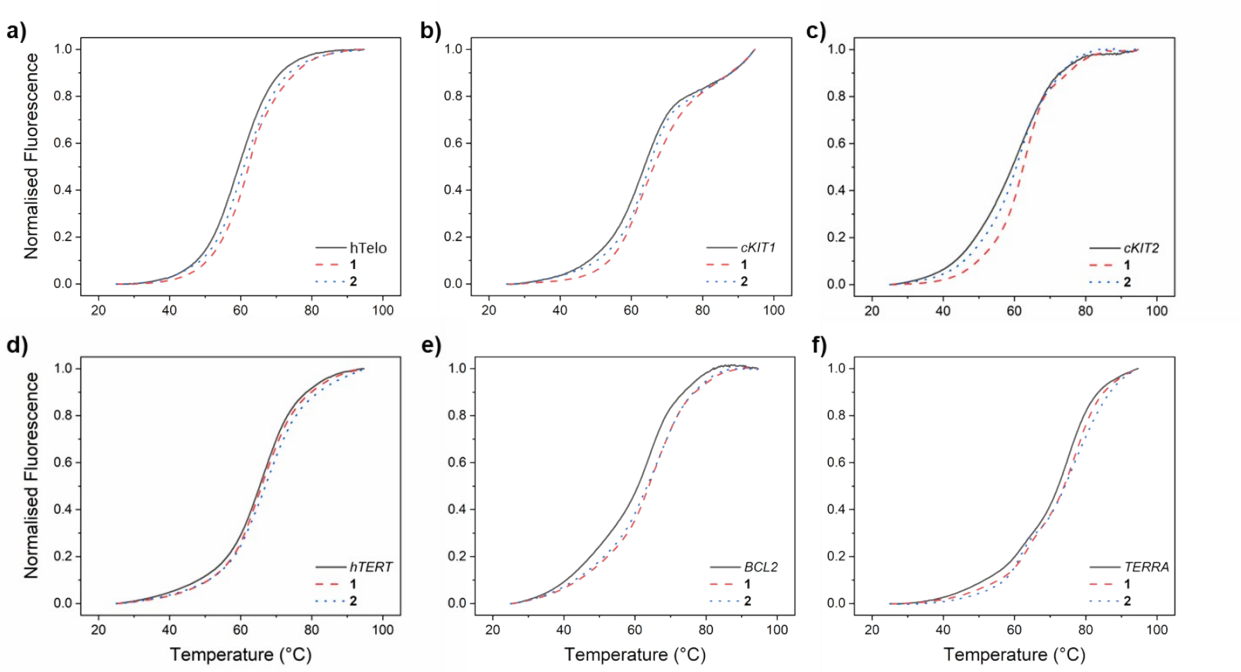


**Figure S18.** Representative FRET melting profiles of 200 nM hTelo (a), *cKIT1* (b), *cKIT2* (c), *hTERT* (d) *BCL2* (e) or *TERRA* (f) G4-DNA alone (black lines) and in the presence of 5 equivalents of the **1** or **2**, in 60 mM KCacodylate buffer (pH = 7.4).

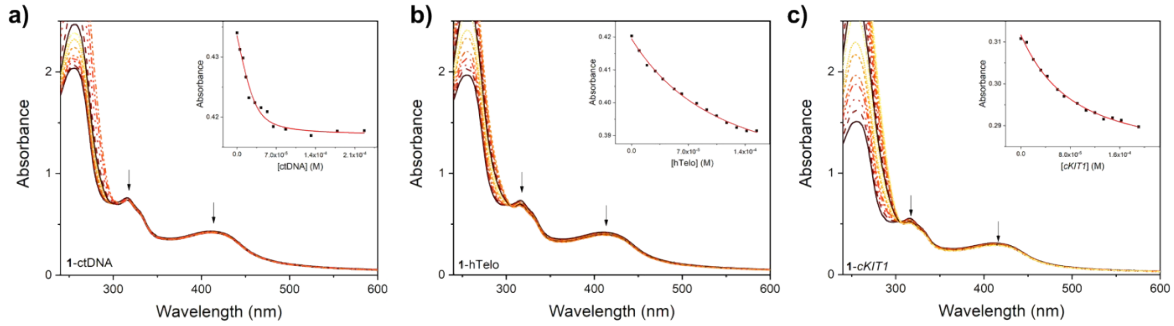


**Figure S19**. UV-Vis spectra of **1** in the presence of increasing amount of DNA collected in 100 mM KCl and 50 mM Tris-HCl buffer. (a) [**1**] = 33.0 μM, [ctDNA] = 0.0 – 227.0 μM; (b) [**1**] = 31.0 μM, [hTelo] = 0.0 – 7.0 μM; (c) [**1**] = 23.7 μM, [*cKIT1*] = 0.0 – 8.7 μM. In the inset representative data fits.

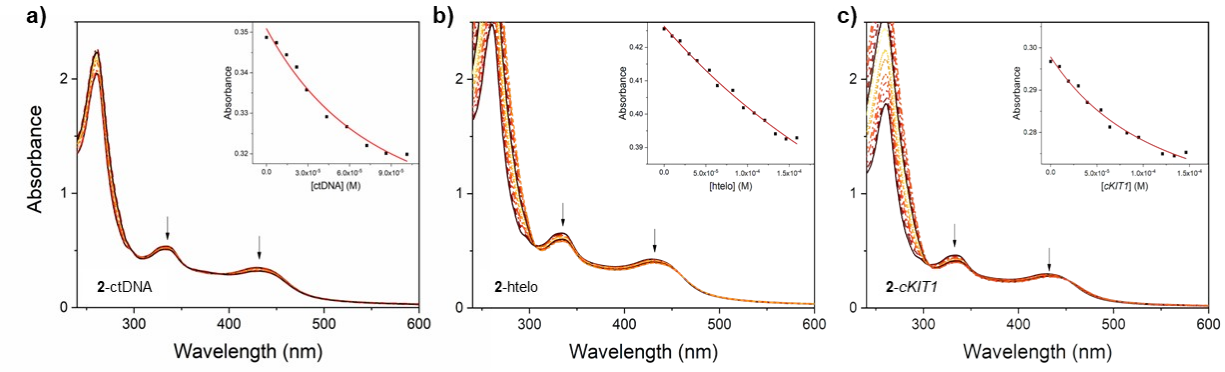


**Figure S20**. UV-Vis spectra of **2** in the presence of increasing amount of DNA collected in 100 mM KCl and 50 mM Tris-HCl buffer. (a) [**2**] = 27.5 μM, [ctDNA] = 0.0 – 101.0 μM; (b) [**2**] = 33.5 μM, [hTelo] = 0.0 –7.2 μM; (c) [**2**] = 23.5 μM, [*cKIT1*] = 0.0 – 6.7 μM. In the inset representative data fits.

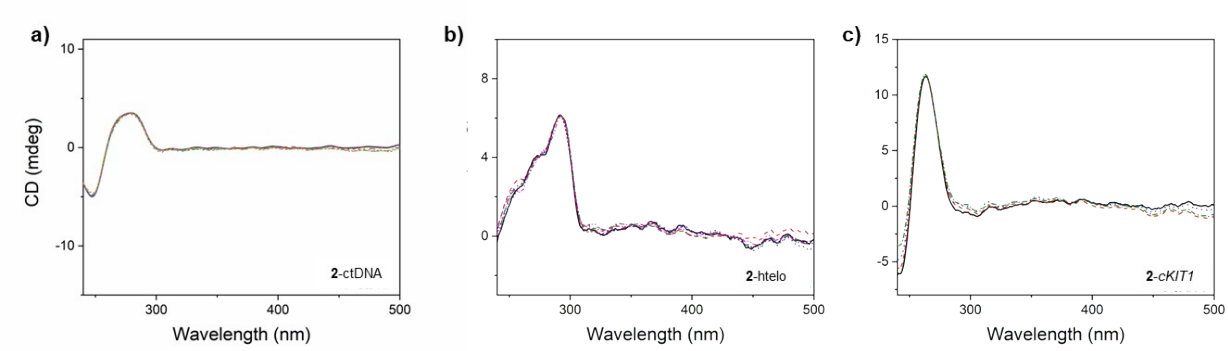


**Figure S21**. CD spectra of duplex- and G4-DNA solutions recorded in 100 mM KCl and 50 mM Tris-HCl buffer, in the presence of increasing amounts of **2**. (a) [ctDNA] = 50.0 μM, [**2**] = 0.0 – 39.7 μM; (b) [hTelo] = 1.5 μM, [**2**] = 0.0 – 8.0 μM: (c) [*cKIT1*] = 1.3 μM, [**2**] = 0.0 – 31.0 μM.

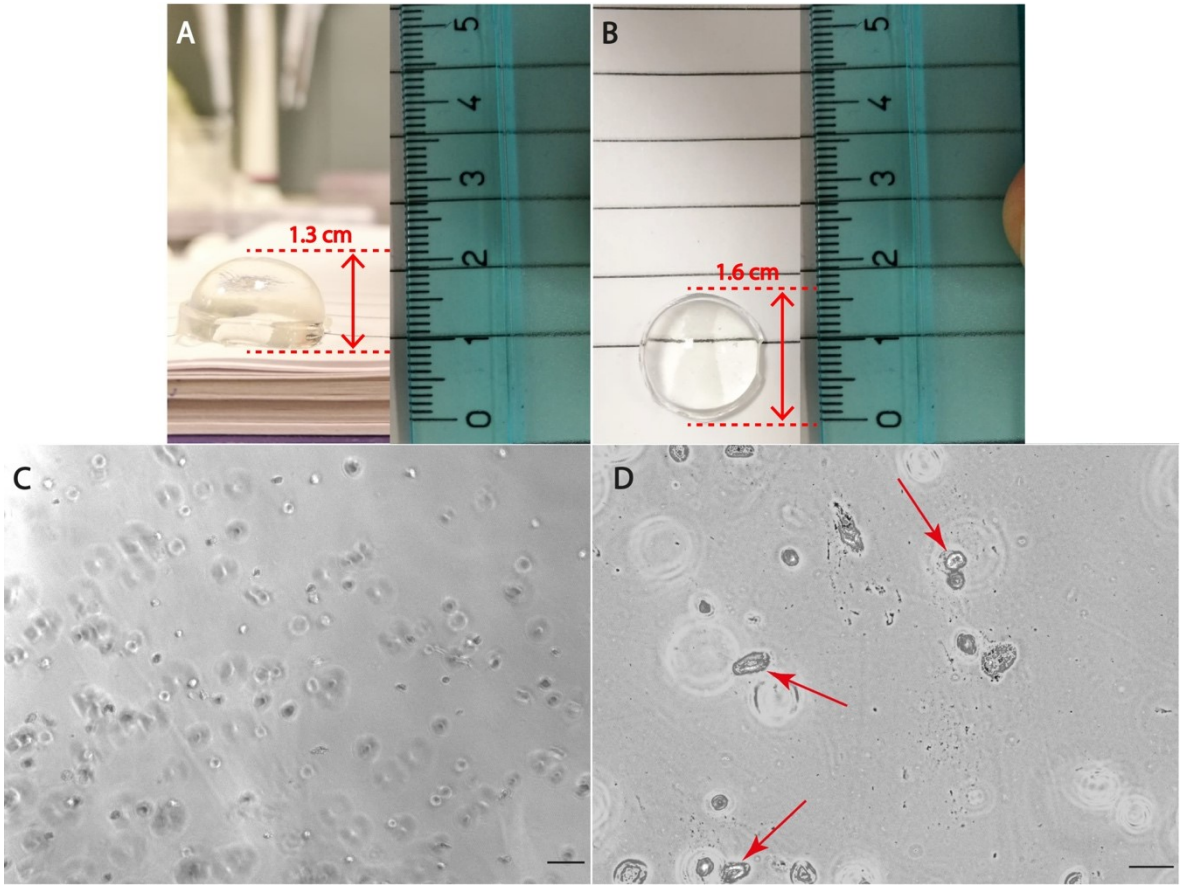


**Figure S22.** Macroscopic image of a GelMA scaffold in frontal (A), and top (B) view. Rounded shaped SW-1353 cells cultured within the scaffold at day 0 (C) and day 7 (D). Pericellular matrix deposition is clearly visible at day 7 (D, red arrows). Scale bar = 50 µm (C) and 25 µm (D).

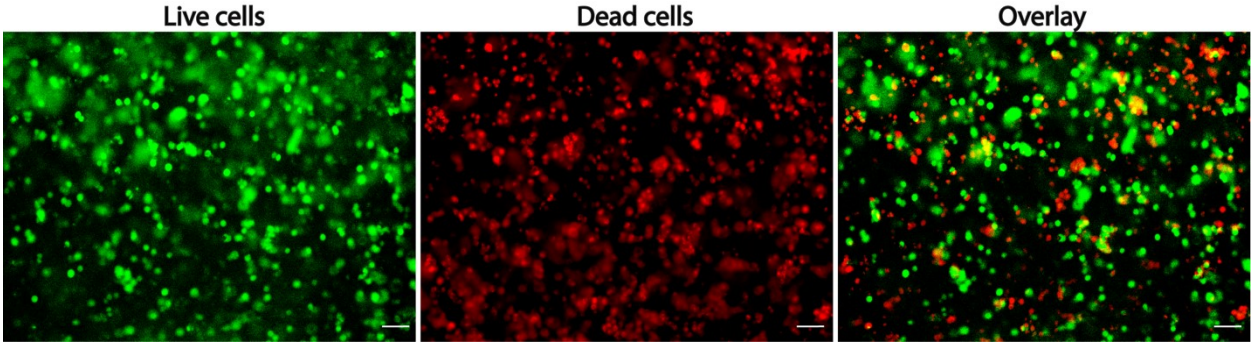


**Figure S23.** Representative images from LIVE/DEAD assay performed on GelMA scaffolds cellularized with SW-1353 cells captured by fluorescence microscopy. The assay relies on a mixture of two fluorescent probes, calcein AM and ethidium homodimer (EthD-1), able to selectively stain live and dead cells respectively. Scale bar = 100 µm.

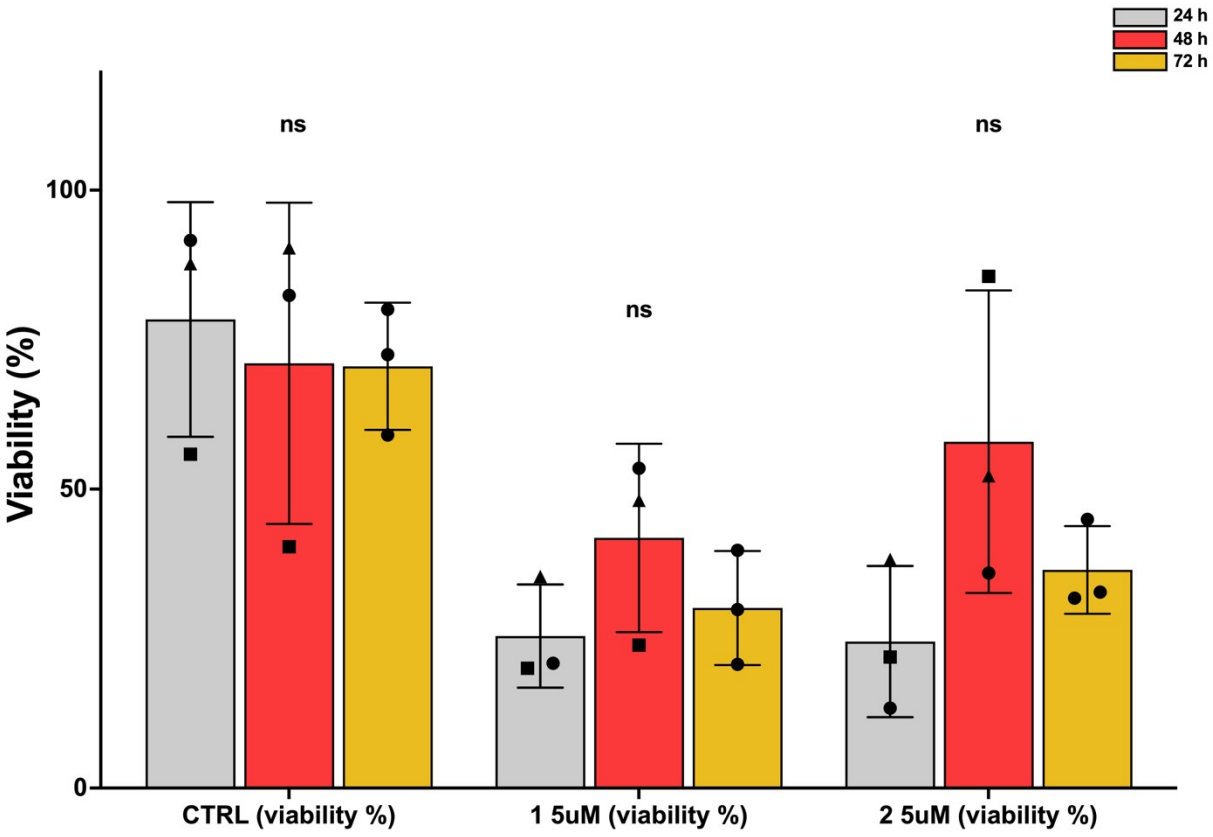


**Figure S24.** Graphical representation of viability data grouped by time-point. Two-way ANOVA followed by Tukey's post-hoc test. Ns = not significant